Acta Cryst. (1984). B40, 21–26

Electron Microscopy and Diffraction of Phases in the Al_2O_3–$BaAl_2O_4$ System

BY N. YAMAMOTO

Department of Physics, Arizona State University, Tempe, AZ 85287, *USA*

AND M. O'KEEFFE

Department of Chemistry, Arizona State University, Tempe, AZ 85287, *USA*

(*Received* 11 *April* 1983; *accepted* 27 *July* 1983)

Abstract

It is shown that two distinct phases exist in the $BaAlO_2$–Al_2O_3 system. One appears well ordered and has symmetry $P6_3/mmc$ and lattice parameters similar to magnetoplumbite or β-alumina phases. The second phase has a supercell $\sqrt{3}a \times \sqrt{3}a \times c$ and is incompletely ordered. The two phases are observed to intergrow coherently.

Introduction

A large number of compounds are known to have structures related to those of β-Al_2O_3 (ideal formula $NaAl_{11}O_{17}$) and magnetoplumbite (ideal formula $BaFe_{12}O_{19}$) (Verstegen & Stevels, 1974; Morgan & Cirlin, 1982). A striking feature of most systems studied is that there is an apparently wide range of composition which does not include the ideal stoichiometry. The ideal structures are characterized by hexagonal symmetry (space group $P6_3/mmc$) and have slabs of oxygen and aluminum (or other bivalent metal such as gallium or iron) between the mirror planes. These slabs have a local structure similar to that of spinel – the 'spinel blocks'. The two structures differ in the arrangement of ions on the mirror planes (Adelsköld, 1938). Following Morgan & Cirlin (1982), the two ideal structures can be written symbolically as

$$\beta\text{: } M^{+}O[Al_{11}O_{16}]$$

$$\text{MP: } M^{2+}AlO_3[Al_{11}O_{16}],$$

where the brackets enclose the spinel blocks and the other atoms lie on the mirror planes (often called the 'conduction planes' in the case of β-aluminas).

Until recently compounds in the MO–Al_2O_3 systems with M = Ca, Sr, Ba or Pb were assigned the ideal MP structure and composition ($MAl_{12}O_{19}$) (Torkar, Krischner & Moser, 1965). However, Verstegen & Stevels (1974) suggested that the structure of '$BaAl_{12}O_{19}$' might be more closely related to that of β. Verstegen (1973) also reported that, for $BaGa_{12}O_{19}$, reflections $00l$ with l odd were observed, ruling out the $P6_3/mcm$ symmetry. Subsequent work (Stevels, 1978) indicated a wide range of stoichiometry for this phase with Ba/Al ranging from approximately 1/8 to 1/17, and it was suggested that crystals might consist of intergrowth of the β and MP structures.

A careful study by Haberey, Oehlschlegel & Sahl (1977) suggested the existence of two distinct phases with Ba/Al equal to 1/9·2 and 1/13·2. The presence of two phases was also found by Kimura, Bannai & Shindo (1982). Their results, in good agreement with those of Haberey *et al.* (1977), can be summarized as follows.

Phase I: Ba/Al = 1/14·6, a = 5·5881, c = 22·732 Å.

Phase II: Ba/Al = 1/9·1, a = 5·6003, c = 22·910 Å.

These lattice parameters are close to those expected for the β or MP type of structure. It should be clear that, owing to their near similarity in the two phases, very careful powder diffraction experiments are necessary to distinguish them.

A Ba β''-alumina has also been prepared (Dunn & Farrington, 1980) by ion exchange. In this structure the stacking of the spinel blocks is different from that of the β structure (see *e.g.* Bovin & O'Keeffe, 1980) and part of the Al is replaced by Mg.

In the course of a study of microdiffraction and microanalysis at the sub-unit-cell level (Spence & Lynch, 1982), the existence of two phases in a sample of nominal stoichiometry $BaAl_{12}O_{19}$ was clearly revealed by electron microscopy. In the present work we have done more electron microscopy on this system in an effort to elucidate further the crystal chemistry and phase relationships in this important class of materials.

Experimental

Specimens with varying Ba: Al ratios ranging from 1:24 to 1:4 and 1:2 were made using standard ceramic methods from (analyzed) finely divided $Al_2O_3 \cdot xH_2O$ and $BaCO_3$. The precursors were thoroughly mixed and sintered in air at 1870 K.

0108-7681/84/010021-06$01.50

Samples for electron microscopy were crushed in an agate mortar and fragments floating in an acetone suspension were scooped up onto copper grids covered with a holey carbon film. They were examined in a JEM 200CX electron microscope for observation of high-resolution images and in a Philips 400T microscope equipped with a Kevex energy-dispersive spectrometer for convergent-beam electron diffraction (CBED) and X-ray fluorescence analysis. The peak intensities in the X-ray spectra were integrated using a Tracor Northern multi-channel-analyzer system after background subtraction.

Diffraction patterns and space groups

Two different types of diffraction patterns were observed. We identify these as coming from crystals of type I and type II designated by Kimura *et al.* (1982). These are shown in Fig. 1 for samples in the [0001], [1$\bar{1}$00] and [1$\bar{2}$10] orientations. The type I diffraction patterns reveal hexagonal symmetry with unit-cell parameters close to those previously reported. The [1$\bar{1}$00] zone pattern in Fig. 1 shows systematic absences ($hh2\bar{h}l$) for l odd. The type II diffraction pattern has the strong spots of the type I pattern but in addition the [0001] zone pattern has weak superlattice spots at $(n/3)\{hh2\bar{h}0\}$. The corresponding [1$\bar{1}$00] zone pattern reveals that these 'spots' are actually diffuse rods parallel to [0001]. The intensity and variation along [0001] of the superstructure rods varies from crystal to crystal.

CBED patterns from crystals of the two types in the [0001] and [1$\bar{1}$00] orientations are shown in Fig. 2. The systematic absences in the type I diffraction

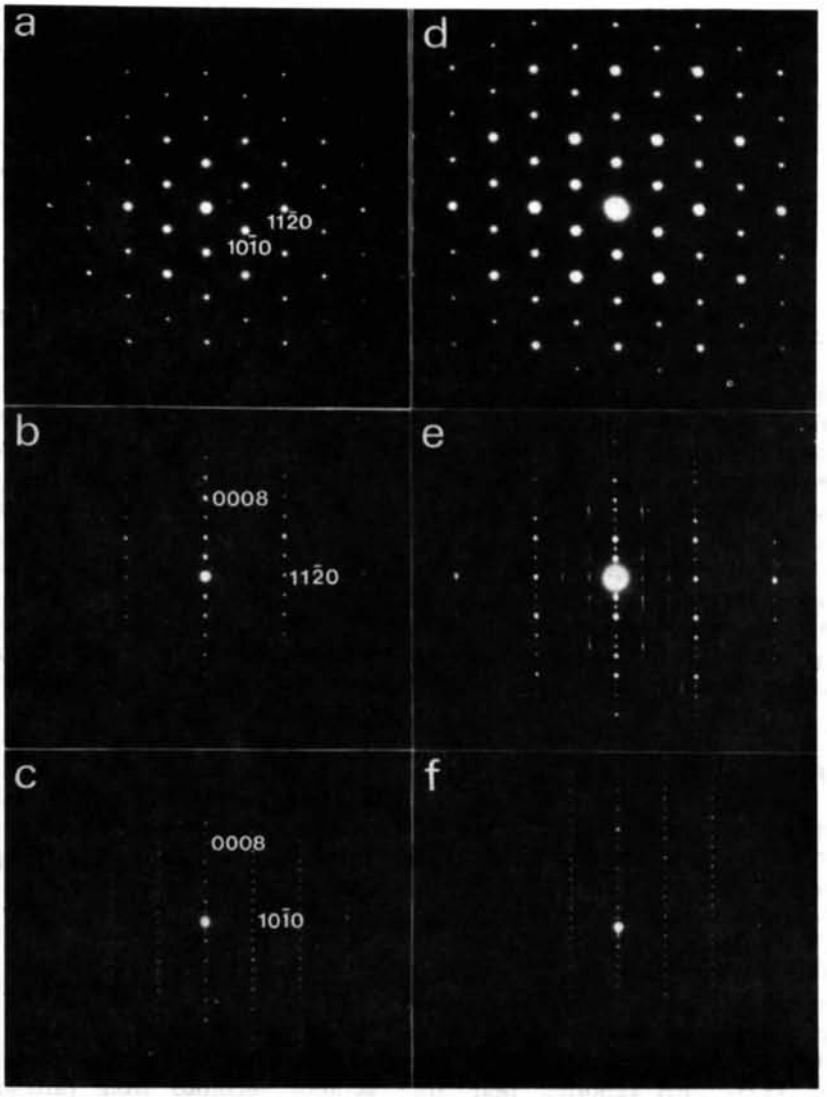

Fig. 1. Diffraction patterns of a type I crystal: (*a*) [0001], (*b*) [1$\bar{1}$00], (*c*) [1$\bar{2}$10]; and of a type II crystal: (*d*) [0001], (*e*) [1$\bar{1}$00] and (*f*) [1$\bar{2}$10]. Zone symbols for type II crystals refer to the lattice of the subcell.

Table 1. *Diffraction-group symmetries for three space groups*

Space group	Point group	Zone axis [0001]	Whole pattern	Dark field
$P\bar{6}2c$	$\bar{6}m2$	$3m1_R$	$3m$	$2mm$
$P6_3mc$	$6mm$	$6mm$	$6mm$	m
$P6_3/mmc$	$6/mmm$	$6mm1_R$	$6mm$	$2mm$

pattern limit the possible space groups to $P\bar{6}2c$, $P6_3mc$ or $P6_3/mmc$. The corresponding point groups are $\bar{6}m2$, $6mm$ and $6/mmm$, respectively. [0001] zone-axis CBED patterns can distinguish between these three symmetries as they will have different diffraction-group symmetries as listed in Table 1 which is abstracted from the table given by Buxton, Eades, Steeds & Rackham (1976). Thus the [0001] CBED pattern of type I has sixfold symmetry of the whole pattern excluding $\bar{6}m2$. The patterns of the $\{hh2\bar{h}0\}$ and $\{h\bar{h}00\}$ reflections at their Bragg positions (as shown in Fig. 3) show $2mm$ symmetry which excludes the possibility of $P6_3mc$. We conclude therefore that the symmetry of the type I phase is $P6_3/mmc$.

It is not easy to determine the symmetry of the type II crystals owing to the presence of disorder (manifest in the diffuse spots); however, the [0001]-zone CBED pattern shows now only a threefold axis in contrast to the sixfold axis of type I and the absence of a mirror plane.

In Fig. 4 we show the relationship between the lattices of type I and type II crystals. The fine solid lines outline the type I lattice and bold solid lines outline unit cells of type II with $a_{II} = \sqrt{3}a_I$. Alternative origins of the unit cell of type II are shown by *A*, *B* and *C*, respectively. Other unit cells in twin orientation with these are also possible, and indeed twinning was often observed in [0001] projection.

High-resolution images

High-resolution images of type I and type II crystals taken with the incident beam parallel to $[1\bar{1}00]$ are shown in Fig. 5. Images changed noticeably in contrast with changes of defocus of about 100 Å. The images in Fig. 5 were recorded at near the Scherzer focus (−660 Å for the 200CX instrument).

The image of type I shown in Fig. 5(*a*) changes from left to right as the crystal was inclined to the incident beam with consequent change of defocus condition across the crystal. The image has a period of $c/2$ along [0001] and $a/2$ along $[11\bar{2}0]$, as expected for crystal symmetry $P6_3/mmc$. However, it is difficult to identify unambiguously the mirror planes – they

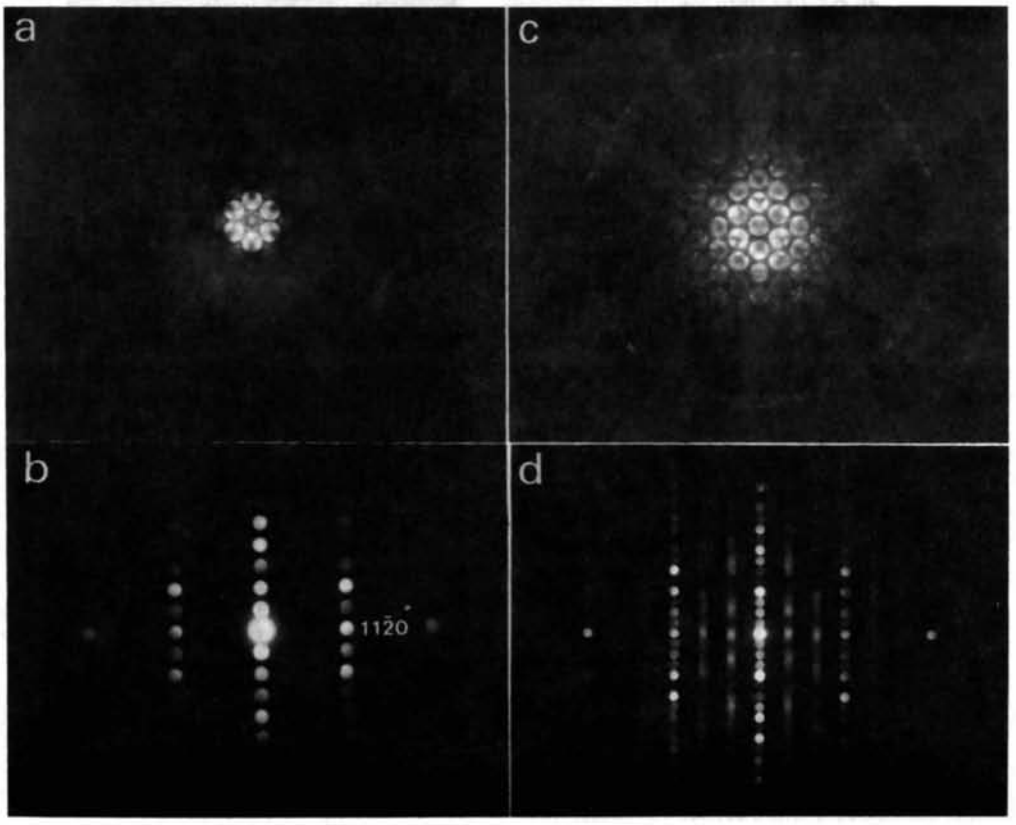

Fig. 2. CBED patterns of type I: (*a*) [0001], (*b*) $[1\bar{1}00]$ and type II crystals: (*c*) [0001] and (*d*) $[1\bar{1}00]$.

could occur at the positions of either the long or the short arrows in the figure.

The image of a type II crystal, shown in Fig. 5(*b*), has twice the period of type I images along [0001] with contrast at alternate local mirrors being very different. The periodicity along [11$\bar{2}$0] is triple that of the type I crystal as expected (*cf.* Fig. 4). Most noticeable is the disorder of the stacking of layers of thickness c along [0001], as also suggested by Fig. 4. Thus, each layer takes one of three different positions (*A*, *B* or *C*) shown in that figure in an almost random order. This is indicated in Fig. 5(*b*) by a stepped line which corresponds to a sequence:

$$\ldots ABBBAABBABCCBAA\ldots.$$

The diffuse lines along the c^* axis in Fig. 1(*e*) are caused by this disorder. Two ordered special cases can be envisaged. The first, $\ldots AAA\ldots$, corresponds to a hexagonal or (more likely) trigonal lattice. The second, $\ldots ABC\ldots$, is monoclinic. Sequences such as $\ldots AB\ldots$ are apparently very rare (*i.e.* *AB* is almost invariably followed by *B* or *C*). Note too that the image detail in each slab of width c is not identical; those slabs indicated by the two arrows have noticeably different images from their neighbors.

Fig. 6 shows a micrograph of a hybrid crystal containing domains of type I and type II crystals coherently intergrown. Rather than sharp boundaries, there is a gradual change of contrast from that typical of one type to that of the other. More complex defects such as stacking faults (*S*) and dislocations (*D*) are also evident. It is interesting to note that after prolonged (10 min or more) exposure to the electron beam images of type II could sometimes be seen to change in part to those characteristic of type I.

This intergrowth image suggests that the structure on one half of the mirror planes of the type II crystals is very similar to that of type I, but that on the other

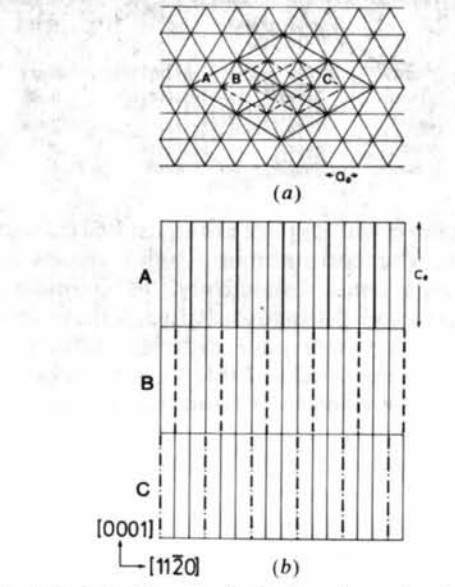

Fig. 4. Relation between the lattices of type I and type II crystals. In (*a*) three possible origins (*A*, *B* and *C*) of the supercell of II with respect to I are shown. In (*b*) an *ABC* sequence of slabs is seen in a projection along [1$\bar{1}$00].

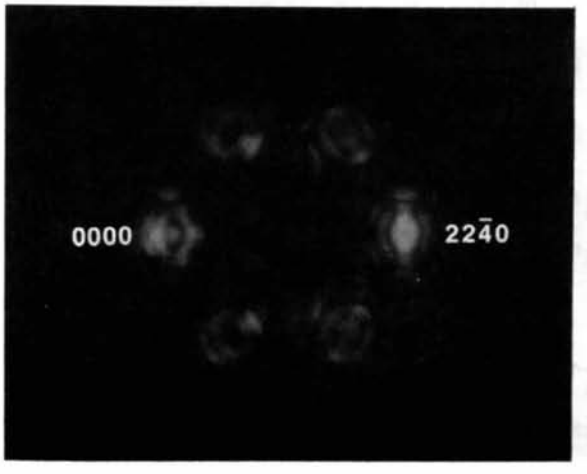

Fig. 3. Dark-field pattern with the Bragg condition satisfied for 22$\bar{4}$0.

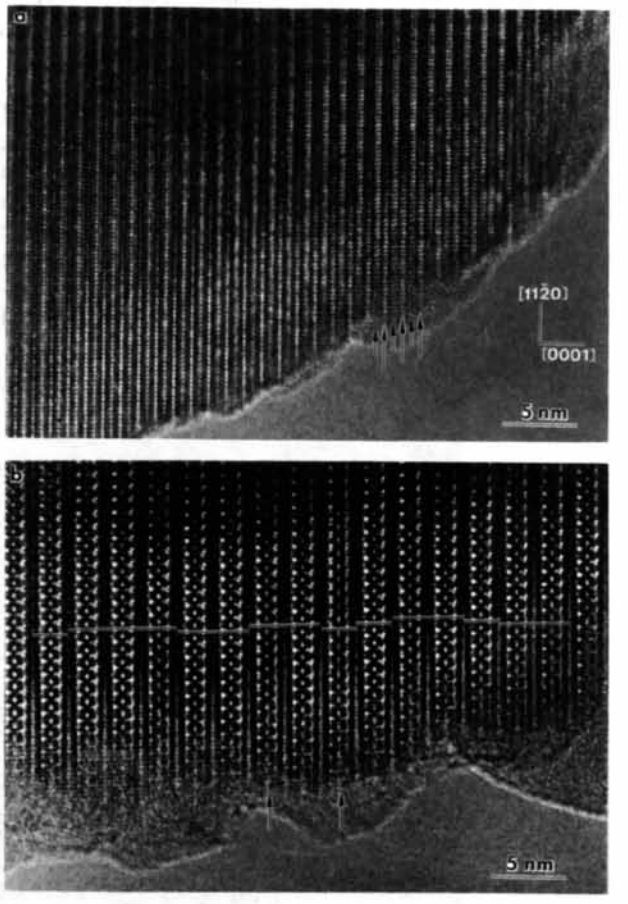

Fig. 5. (*a*) High-resolution image of a type I crystal; (*b*) high-resolution image of a type II crystal with the electron beam parallel to [1$\bar{1}$00] (*cf.* Fig. 4).

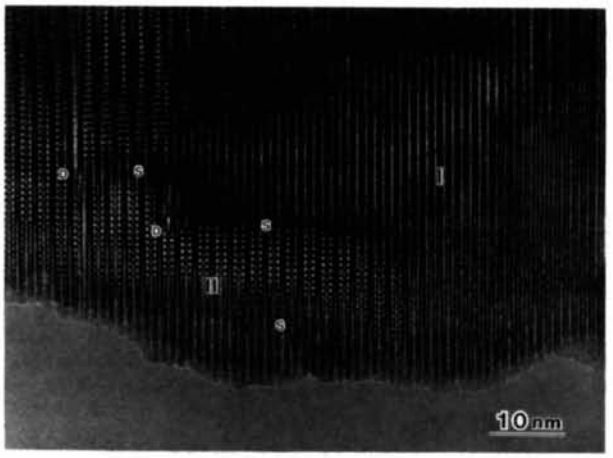

Fig. 6. Micrograph showing intergrowth of type I and type II crystals. Orientation as in Fig. 5.

half there is a very different structure (presumably richer in Ba).

Chemical analyses

X-ray spectra were obtained from thin areas of crystals identified as type I or type II from their diffraction patterns. Typical spectra are shown in Fig. 7 in which the Al and Ba peaks are identified. The different Ba:Al intensity ratios are apparent. For the type I crystals the integrated intensity ratios $I_{Ba}/I_{Al} \simeq 0{\cdot}24$. For type II crystals this ratio was variable between 0·30 and 0·58, with the larger values correlating with the appearance of stronger diffuse superstructure peaks in the $[1\bar{1}00]$ diffraction pattern. Part of the variability might arise from the fact that the illuminated area was normally about 800 Å in diameter and intergrowths of types I and II such as shown in Fig. 5 may well exist. However, even with a 400 Å diameter probe there was still some variability, but with values clustered closer about the maximum value (0·58) quoted above.

To put the analysis on a more quantitative basis the ratio I_{Ba}/I_{Al} was also measured for pure $BaAl_2O_4$ and found to be $2{\cdot}57 \pm 0{\cdot}10$. Thus, if it can be assumed (Cliff & Lorimer, 1976) that $Ba:Al = kI_{Ba}/I_{Al}$, then $k = 0{\cdot}195$. This would make the Ba:Al ratio

$$\text{for type I, Ba:Al} = 1:21,$$

$$\text{for type II, Ba:Al} = 1:8{\cdot}8,$$

where for type II we have used the maximum value of I_{Ba}/I_{Al}. However, the spread of observed values suggests that both phases have variable composition. It also shows that our preparations failed to reach homogeneity (Fig. 8).

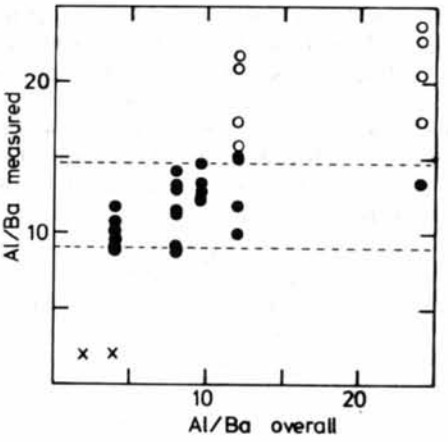

Fig. 8. Observed compositions of crystals as a function of gross composition of the starting preparation. Filled circles type II, open circles type I, cross is $BaAl_2O_4$. The horizontal dashed lines correspond to the compositions reported by Kimura *et al.* (1982) for types I and II.

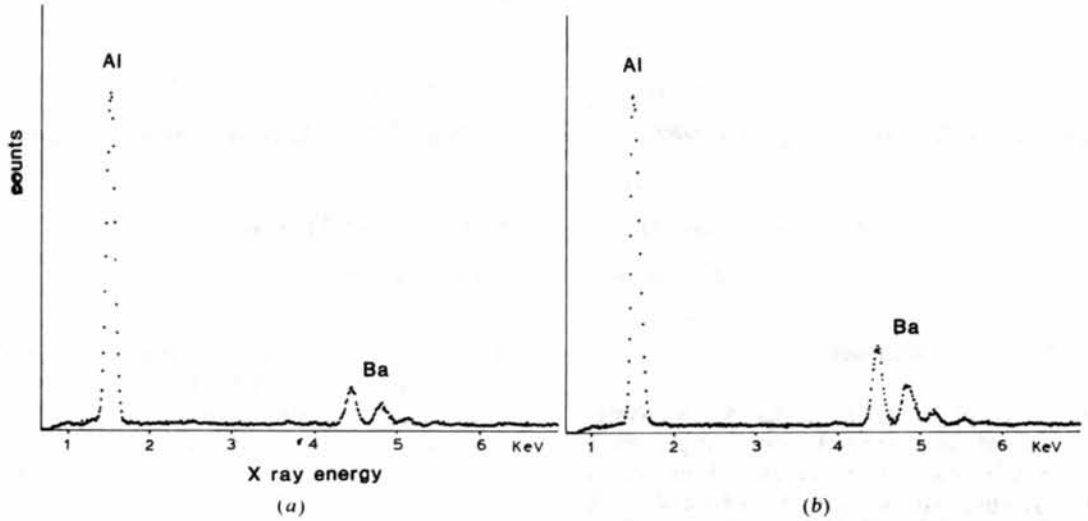

Fig. 7. Typical X-ray spectra from (*a*) type I and (*b*) type II crystals.

Conclusion

The existence of two distinct phases in the BaO–Al_2O_3 system with compositions intermediate between $BaAl_2O_4$ and Al_2O_3 has been clearly demonstrated. The more alumina-rich phase appears to be well-ordered and has a unit cell compatible with the MP or β type of structure, and symmetry $P6_3/mmc$. The second (Ba-rich) phase is found to be completely disordered, but there is clear evidence for a $\sqrt{3}a \times \sqrt{3}a$ supercell ordering in alternate mirror planes perpendicular to the c axis, with, however, imperfect ordering of the slabs along the c axis. Evidence for ordering in β''-aluminas has been found before (Boilet, Colin, Colomban & Comes, 1980), and Hansen & Bovin (1982) have found that a natural plumboferrite (nominal composition $PbFe_4O_7$) has diffraction patterns and images similar to those recorded here for phase II. Since this work was completed, Morgan & Shaw (1983) and Iyi, Takekawa, Bando & Kimura (1983) have also presented new evidence for the existence of two distinct phases in the $BaAl_2O_4$–Al_2O_3 system.

The ready intergrowth of the two phases suggests that conventional methods of phase and structure analysis in these and related systems may fail and that further electron optical studies are called for in other systems. These are in progress.

We are grateful to Drs J. C. H. Spence and J. Lynch, who first observed phases I and II by electron microscopy, for calling our attention to this problem, and to T. R. Wagner for some of the preparations. This work was supported by ARO contract DAAG29-80-C-0080 and by grant DMR-8119061 from the National Science Foundation and made use of the NSF HREM facility at Arizona State University.

References

ADELSKÖLD, V. (1938). *Ark. Kemi, Mineral. Geol.* **12A**, 1–9.
BOILET, J. P., COLIN, G., COLOMBAN, P. & COMES, R. (1980). *Phys. Rev. B*, **22**, 5912–5923.
BOVIN, J. O. & O'KEEFFE, M. (1980). *J. Solid State Chem.* **33**, 37–41.
BUXTON, B. E., EADES, J. A., STEEDS, J. W. & RACKHAM, G. M. (1976). *Philos. Trans. R. Soc. London Ser. A*, **281**, 171–194.
CLIFF, G. & LORIMER, G. W. (1976). *Proceedings of the 5th European Congress on Electron Microscopy*, p. 140. Bristol: Institute of Physics.
DUNN, B. & FARRINGTON, G. C. (1980). *Mater. Res. Bull.* **15**, 1773–1777.
HABEREY, F., OEHLSCHLEGEL, G. & SAHL, F. (1977). *Ber. Dtsch. Keram. Ges.* **54**, 373–378.
HANSEN, S. & BOVIN, J.-O. (1982). *Electron Microscopy* 1982, Vol. 2, pp. 27–28. Frankfurt: Deutsche Gesellschaft für Elektronenmikroskopie.
IYI, N., TAKEKAWA, S., BANDO, Y. & KIMURA, S. (1983). *J. Solid State Chem.* **47**, 34–40.
KIMURA, S., BANNAI, E. & SHINDO, I. (1982). *Mater. Res. Bull.* **17**, 209–215.
MORGAN, P. E. D. & CIRLIN, E. H. (1982). *J. Am. Ceram. Soc.* **65**, C114–C115.
MORGAN, P. E. D. & SHAW, J. M. (1983). *Mater. Res. Bull.* **18**, 539–542.
SPENCE, J. C. H. & LYNCH, J. (1982). *Ultramicroscopy*, **9**, 267–276.
STEVELS, A. L. N. (1978). *J. Lumin.* **17**, 121–133.
TORKAR, K., KRISCHNER, H. & MOSER, H. (1965). *Monatsh. Chem.* **96**, 423–429.
VERSTEGEN, J. M. P. J. (1973). *J. Solid State Chem.* **7**, 468–473.
VERSTEGEN, J. M. P. J. & STEVELS, A. L. N. (1974). *J. Lumin.* **9**, 406–414.

Acta Cryst. (1984). B**40**, 26–38

The Structure of $[Er(1)_{1-x}, Sn(1)_x]Er(2)_4Rh_6Sn(2)_4Sn(3)_{12}Sn(4)_2$, a Ternary Reentrant Superconductor

BY J. L. HODEAU AND M. MAREZIO

Laboratoire de Cristallographie, CNRS, Associé à l'USMG, BP 166*X*, 38042 *Grenoble, France*

AND J. P. REMEIKA

Bell Laboratories, Murray Hill, New Jersey 07974, *USA*

(*Received* 17 *January* 1983; *accepted* 2 *August* 1983)

Abstract

The structure of phase II in the Er–Rh–Sn system has been solved and refined from single-crystal X-ray diffraction data. It is described in the tetragonal system, space group $I4_1/acd$, with eight formulae per unit cell of dimensions $a = 13{\cdot}73$ and $c = 27{\cdot}42$ Å. The chemical formula is $[Er(1)_{1-x}Sn(1)_x]Er(2)_4Rh_6Sn(2)_4Sn(3)_{12}Sn(4)_2$, where Rh and Sn(3) correspond to two and four different crystallographic sites, respectively. All crystals are twinned by reticular pseudomerohedry. The atoms occupy the following positions: $M(1) \equiv [Er(1)_{1-x}Sn(1)_x]$ in $8(b)(00\frac{1}{4})$; $Rh_{[1]}$ in $16(d)(00z)$;

0108-7681/84/010026-13$01.50